HAL
open science

Beyond the paradigm of nanomechanical measurements on cells using AFM: an automated methodology to rapidly analyse thousands of cells

S. Proa-Coronado, Childérick Séverac, A. Martinez-Rivas, Etienne Dague

To cite this version:

S. Proa-Coronado, Childérick Séverac, A. Martinez-Rivas, Etienne Dague. Beyond the paradigm of nanomechanical measurements on cells using AFM: an automated methodology to rapidly analyse thousands of cells. Nanoscale Horizons, 2020, 5 (1), pp.131-138. 10.1039/C9NH00438F . hal-03025101

HAL Id: hal-03025101

https://laas.hal.science/hal-03025101v1

Submitted on 26 Nov 2020

HAL is a multi-disciplinary open access archive for the deposit and dissemination of scientific research documents, whether they are published or not. The documents may come from teaching and research institutions in France or abroad, or from public or private research centers.

L'archive ouverte pluridisciplinaire **HAL**, est destinée au dépôt et à la diffusion de documents scientifiques de niveau recherche, publiés ou non, émanant des établissements d'enseignement et de recherche français ou étrangers, des laboratoires publics ou privés.

Beyond the paradigm of nanomechanical measurements on cells using AFM: An automated methodology to rapidly analyse thousands of cells.

S. Proa-Coronado,[a,b,c,d] C. Séverac,[b] A. Martinez-Rivas,[a,c,Ø,*] and E. Dague[d,Ø,*]

1. ENCB-Instituto Politécnico Nacional (IPN), Av. Wilfrido Massieu, Unidad Adolfo López Mateos, 07738, Mexico City, Mexico
2. ITAV-CNRS, Université de Toulouse, CNRS, Toulouse, France
3. CIC-Instituto Politécnico Nacional (IPN), Av. Juan de Dios Bátiz S/N, Nueva Industrial Vallejo, 07738, Mexico City, Mexico
4. LAAS-CNRS, Université de Toulouse, CNRS, Toulouse, France
Ø. Equal contribution
*: nanobiomed@hotmail.com, edague@laas.fr

Abstract

Nanomechanical properties of cells could be considered as cellular biomarkers. The main method used to access the mechanical properties is based on nanoindentations measurements, performed with an operator manipulated Atomic Force Microscope (AFM) which is time-consuming, and expensive. This is one of the reasons preventing the transfer of AFM technology into clinical laboratories. In this paper we report a methodology which includes an algorithm (transferred to a script, executed on a commercial AFM) able to automatically move the tip onto a single cell and through several cells to record force curves combined with a smart strategy of cell immobilization. Cells are placed into microwells of a microstructured polydimethylsiloxane (PDMS) stamp. Inside a classical 100x100 µm^2 AFM field, 100 cells can be immobilized. In an optimal configuration we were able to measure, within 4 h, a population of 900 *Candida albicans* cells both native and caspofungin treated, which represents an unprecedented performance. We discovered that the population is heterogeneous and can be divided, on the basis of nanomechanical properties, into 2 subgroups.

Introduction

Medical doctors constantly have to face the issues of diagnostic, prognostic or evaluation of treatment efficiency. To tackle this question there is a constant need to develop and adapt new, more accurate and sensitive biomarkers, able to help in differential diagnostic or be predictive as early as possible of the disease evolution. In this aspect cell mechanical properties have the potential of being used as label free biomarkers for some pathologies[1]. Indeed, cell mechanical properties have the potential to address the diagnostic of cancer[1–4] as it has been reported that cancerous cells change their mechanical phenotype, presenting a lower Young modulus[5–7] and adhesion[7–9] than normal cells. Other authors have reported that cell mechanical properties are modified during proliferation[10], by comparing their elastic modulus to differentiate normal cells from cancerous cells[11] or normal cells from cells treated for example with H_2O_2, N-ethylmaleimide and chymotrypsin[12]. In the field of cardiology, it is also known that erythrocytes interactions with fibrogen, as probed by AFM, are modified in ischemia and that red blood cells stiffness is altered[13]. As for the cardiology

area for example cardiomyocytes are difficult to handle, and then works have reported the characterization of 1 to 30 cardiomyocytes[14–20] in about 6-8 h. which is a too small amount of cells to make a statistically relevant information in the context of human diseases and therefore will never be reliable enough for clinicians. Mechanical properties have also help understanding the effects of antimicrobial molecules on bacteria or yeast cell's walls[21]. Another example in the bacteria field is the work of Francius et.al[22]. They reported that *S. aureus* exposed to lysostaphin, presented a decrease in elasticity and stiffness of its cell membrane. Also, Feuillie et.al[23] reported in their paper that when treating bacteria with a peptide derived from β-neurexin, it blocks the surface protein SdrC which impacts on the cell adhesion. Formosa et.al[24] reported the increase of the cell wall elastic modulus and an overexpression of the adhesive protein Als1p when exposing *Candida albicans* to some incremental doses of caspofungin. Mechanical properties help understanding the microorganisms cell wall structure, their resistance mechanisms, and adhesion processes[25,26].

Atomic Force Microscopy (AFM)[27] is the technique of reference to acquire mechanical properties of cells[28,29]. The classical procedure to obtain force curves from an AFM can be described by the following steps: first the tip is calibrated, then the sample is placed on the microscope stage, next a topographic image is acquired to determine the position of the cells, the tip is moved to the central region of each cell. AFM indentations at different locations of the cell are performed, and force curves are obtained and recorded. Finally, when all the cells are measured, the stage is moved so that new cells are brought into the AFM field of view. This cycle is performed manually, and its throughput is low (<1 cell/10 min.)[30]. Up to this time the technique is neither used in the pharmaceutical industry nor in the antimicrobial drug discovery process. AFM is perceived as a research tool and indeed, the works reported so far have one common factor, which is the limited number of cells analyzed by an AFM. This limited number prevents the analysis of a cell population and therefore prohibits statistically relevant general conclusions or decisions. To be able to transfer the AFM technology to hospitals or pharmaceutical industry a mandatory step is to achieve high throughput results in order to analyze cell populations rather than single cells[21,31].

Wang et.al[32] developed an automated system which uses image processing to identify Raji cell locations so the AFM tip can move exactly above the cells and take measurements. The location and measurement of the cells are done within 3 s per cell, but their system had some requirements: the cells needed to be round shape (which is usually the sign of dying cells), as the algorithm could only recognize round shape cells confining the system to a specific cell geometry. Moreover, the cells substrate had to be completely flat and the agglomeration of cells were to be avoided, because the system did not withdraw the tip from the sample. Finally, the authors tested their system with 4 cells per scanning area, but they did not report the number of cells analyzed per hour. In another effort to develop AFM measurements on tissues Roy et.al[33] developed a system that used image processing to align the AFM probe with a tissue of interest, they were able to obtain in an area of 80 µm x 150 µm up to 480 force curves in ~80 min. Nevertheless, the aim of their semi-automated system consisted in analyzing changes in tissue architecture not being adapted for single cell analysis. Another approach reported by Favre et.al[34], focused on maximizing the number of cells analyzed by AFM. They developed an array of cantilevers that are controlled by one AFM acquiring images from different regions of a sample at the same time. However, to

apply this technology to a cell population the cantilever arrays should be fabricated with the same dimensions as the cell arrays. Another example was the parallelism of AFM which was reported by Sadeghian et.al[35]. Their tool involved the miniaturization of AFMs, they reported a maximum of 44 miniaturized AFM in an area of 450 mm (wafer like area). Each AFM was capable of working independently from the others having different kinds of analysis. The authors tested the system by obtaining topographical images of colloidal gold nanoparticles (10 nm in diameter) deposited on mica. However, the AFM heads distribution is very particular, and the cell array had to be adapted. Moreover, the regions of interest locations are determined manually, meaning that the human intervention is still predominant. Both parallel solutions did not consider a way to automatically bring new cells (or another cell array) inside the field of view of the AFM, consuming a vast amount of time.

Very recently Antoine Dujardin et.al[36] reported a solution where an automated procedure allows an AFM to obtain biomechanical analysis on prokaryotes. A python script was implemented in a Dimension Fast Scan-Bio AFM (Bruker, Santa Barbara, CA, USA), however this process takes considerable time to realign the photodetector and perform the engagement each time to finally analyze 501 areas in 8 h 35 min. They tested the system with fixed *Yersinia pseudotuberculosis* and living *Mycobacterium bovis* BCG bacteria. To identify the bioelements, a force volume image was performed in each well. This image was used to determine the bacteria positions (on the basis of their height) and the identified positions were imaged (2x2 μm^2 area). The reported images are height and Peak Force-error signals discarding the option to perform a mechanical analysis on the analyzed bacteria.

In the present work an original automated methodology, previously submitted as patent[31] to measure cellular mechanical properties is reported. Our methodology combines a purposely developed copyright algorithm[37] executed as a script on commercial AFMs with a smart strategy of cell immobilization (supp. Figure S2). The script automatically moves the tip from cell to cell to record force curves of each cell of a cell population. Cells are immobilized at known locations into microwells of a microfabricated PDMS stamp[38]. Once the tip has scanned all the cells of the scanning area, a motor stage moves automatically and brings a new cell array into the scanning area to re-initiate the methodology.

We tested this AFM based automated methodology on eukaryotes *C. albicans* because they are known as an opportunistic pathogenic yeast which represents one of the main hospital-acquired infections. We decided to compare native *C. albicans* cells with caspofungin treated *C. albicans* cells. Caspofungin is a last change antifungal drug form the echinocandin class, know to modify the yeast cell wall mechanical properties[24]. In our test, the automated methodology takes an average time of 12 seconds to perform 9 nanoindentations per cell and per microwell, giving a large number of force curves that is between 8,000 to 9,000 in 4 h, providing a method for high throughput measurements of a cell population. This automated process can be considered as the first step for a viable future diagnostic tool[31]. Thanks to this development we present for the first time the mechanical properties of a cell population (800-900 cells) measured by AFM pointing out that the mechanical properties within the cell population is not homogeneous and may explain conflicting results from literature.

Results and discussion

Figure 1 shows the execution of the program developed for this work (recommendations to initialize the algorithm: supp. figure S1 and description of the algorithm in supp. Figure S2 and supp. Figure S3), 1A and 1B shows how the cantilever moves from one scanning area to another. The centering algorithm takes ~40 s to be executed on each microwell. Figure 1C shows the displacement among the microwells in one scanning area, the movement is from the center of one microwell to the center of other microwell. The program takes ~12 s to finish the 9 indentations per microwell and ~13 min. per area, that is 64 wells per scanning area. Then Figure 1D shows the nanoindentation on different regions inside a microwell. This result can be seen in the video on the supp. data information.

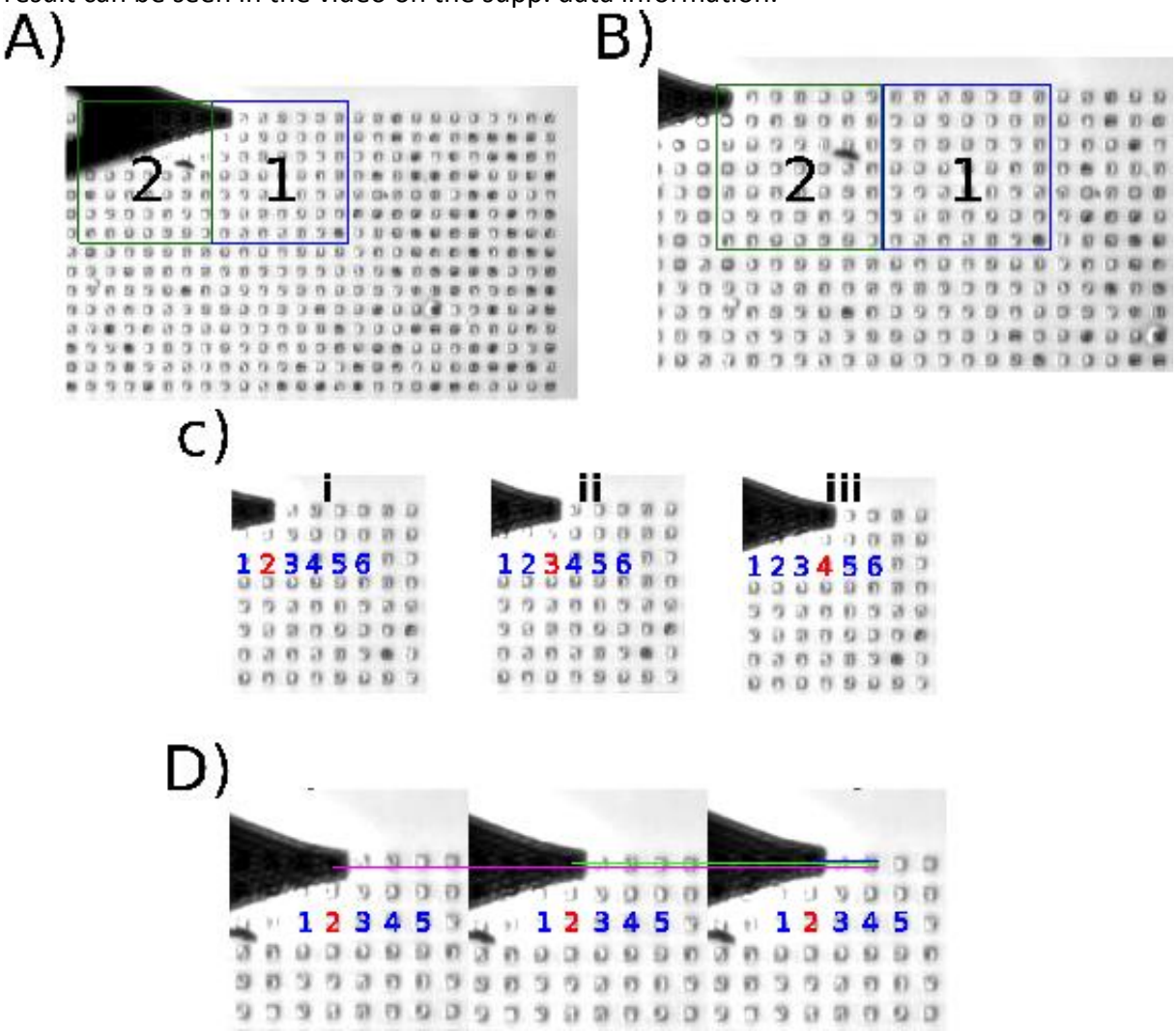

Figure 1. Algorithm execution. Screenshots taken from the Supp data video. A: Location of the center of the first microwell in the current scanning area. B: Position of the tip after moving the motor stage, area 2 is the active scanning area at this moment. C: Shows the data acquisition through different microwells (i-iii). D: Shows the data acquisition inside one microwell, the indentation is performed in different regions of the same microwell (magenta/green/blue).

The force curves were obtained from *C. albicans* cells immobilized inside the micro-fabricated wells. Four experiments were conducted with the objective to establish the repeatability and reliability of the results. Native and caspofungin treated cells were independently prepared as mentioned in the materials & method section and immobilized the day they were used. The decision to use caspofungin is because its action on the yeast

cell wall is still under debate[24,42]. The script was executed and 1021 cells were analyzed for the first experiment (native cells), 957 cells for the second experiment (native cells), 1000 cells for the third (caspofungin), and 574 cells for the fourth experiment (caspofungin). For the experiments 1 and 3, 16 indentations per cells were taken, meanwhile for experiments 2 and 4, 9 nanoindentations were taken.

Experiments 1, 2, 3, and 4 are independent duplicates. The cell cultures were independent and were not performed the same day. Four experiments were performed, two of them (experiments 1 and 2) with native cells and two (experiments 3 and 4) with caspofungin treated cells. The objective of this setup was to obtain a comparable number of analyzed cells (for native and treated) and to determine the maximum number of cells analyzed in a fixed time (4 h).

Following the previous criteria Table 1 presents the number of cells analyzed, the number of force curves discarded, and the time taken to analyze each well.

Table 1. Summary of the information derived from the experiments.

	Experiment	Force Curves	Wells analyzed	Cells analyzed	Time per well(s)	Discarded force curves (%)
Native cells	1	15927	1021	1021	9	4.31
	2	8620	959	957	12	12.87
Treated cells	3	15457	1018	1000	9	8.19
	4	5180	579	574	12	20.88

The force curves obtained were analyzed using the JPK data processing software, based on the work published by El-Kirat-Chatel[42] we extracted the cell spring constant from all the force curves. However, the filling rate of the PDMS stamp is not 100 % (actually ~86 %). In the sup. data section dealing with force curves acquisition and analysis, the parameters used to exclude curves recorded out of the cells are described (supp. Figure S4). To filter the force curves the following criteria was implemented:

- The contact point is used to determine if the force curves are from the bottom of the well, so all the curves with a contact point value below 4.15 µm are discarded.
- Curves with a negative slope are discarded.
- We assumed that the cell spring constant should be lower than that of the PDMS measured at 150 pN/nm, hence we discarded all force curve giving a spring constant higher than 150 pN/nm.

Figure 2 presents the spring constant and adhesion histograms for *C. albicans* cells in native conditions (A and B) and treated with caspofungin (C and D). 2A and B, left, show the spring constant histograms, the number of cells analyzed in the first two experiments were 1021 and 959 respectively; both are obtained by analyzing independently the cultured native cells. Analyzing the two histograms with the k-means method they can be deconvoluted into 2 populations that are slightly different in the 2 experiments. The first population has a mean

spring constant of 21 ±6 pN/nm (experiment 1) and 30 ±13 pN/nm (experiment 2) while the second population has a spring constant of 48 ±9 pN/nm (experiment 1) and 80 ±18 pN/nm (experiment 2). For the experiments 3 and 4 (Figure 2C and D, left) 1018 and 579 cells were analyzed. According to the literature[42], treated cells present a softening of the cell wall because of the caspofungin treatment.

This shift can be seen in Figure 2, comparing experiments 1 and 3. The peak present at 21 pN/nm (2A-left) shift to 13 pN/nm (2C-left) and the peak at 48 pN/nm shifts to 42 pN/nm. For experiments 2 and 4 (2B and 2D, -left, respectively) the peak present at 30 pN/nm shifts to 15 pN/nm and the peak at 80 pN/nm shifts to 52 pN/nm. Figure 2E and 2F show the one-way ANOVA test, 2E-left was obtained comparing 2A and 2C spring constant data reducing both sets to 1018 cells, meanwhile 2F-left was obtained by comparing 2B and 2D spring constant data reducing both sets to 579. The one way test is used to compare the native cells results against treated cells obtaining a p<0.001 (represented by ***).

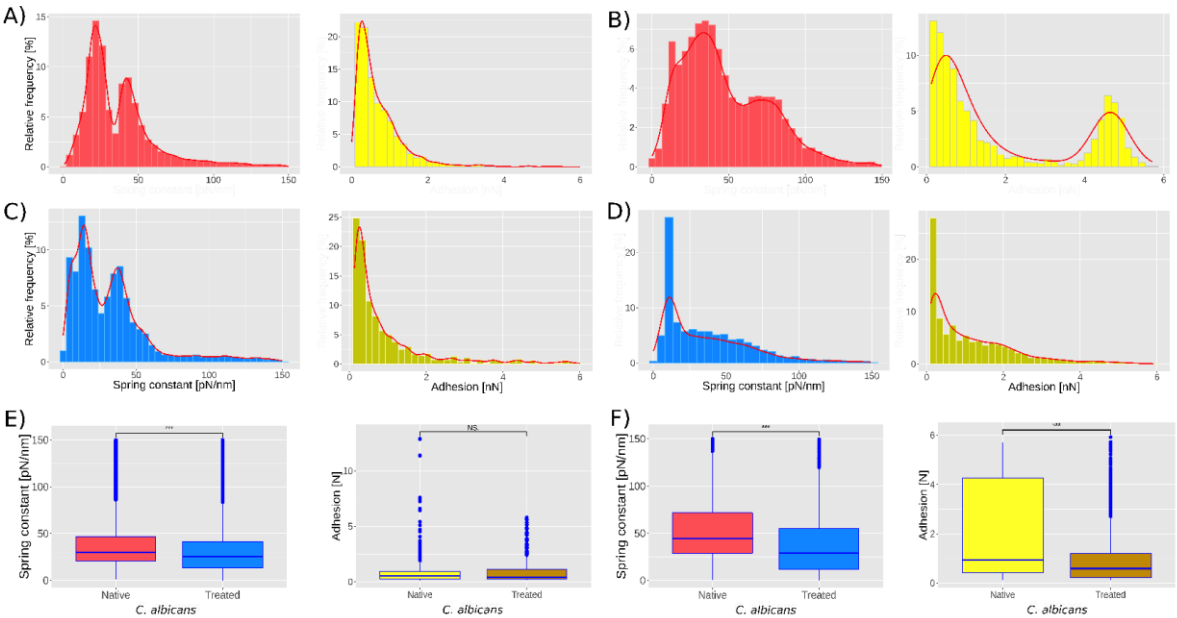

Figure 2. *Spring constant histograms for C. albicans, native and treated with caspofungin. A and B (left) show the spring constant histograms for experiments 1 and 2 of native C. albicans cells (1021 and 959 cells analyzed respectively). While C and D (left) show the spring constant histograms for the experiments 3 and 4 of treated C. albicans cells (1018 and 579 cells analyzed respectively). A and B (right) show the results obtained from the adhesion analysis on experiments 1 and 2. C and D show the adhesion results for experiments 3 and 4. E and F show the one-way ANOVA test performed using the spring constant and adhesion data from 1-3 and 2-4 respectively. *** = p value < 0.001, NS = no significant difference. Bin width was determined by Freedman-Diaconis rule.*

Figure 2A-right shows that the adhesion force between the bare tip and native cells was 0.64 ±0.6 nN in the first experiment, while in the second experiment still on native cells, 2 subpopulations were found: the first has a mean adhesion force of 0.7±1.4 nN while the second is 4.5±1.5 nN. The treatment with caspofungin has no significant effect on the adhesion if experiment 1 and 3 are considered (one way ANOVA test, figure 2E-right shows no significant difference) but it seems that caspofungin induces a decrease in the adhesion to the tip and a reduction of the population adhesion heterogeneity.

Discussion

The protocol used to immobilize the cells is the one described by Formosa et. al[38], nevertheless in this work a modification was made to go from ~50 % to ~85 % of microwells filled with cells (see materials & methods section). The number of nanoindentations were 16 for experiments one and three and 9 for experiments two and four. The objective of varying the number of nanoindentations was to observe if a significant change will be present in the histograms, and as can be seen the two subpopulations start to merge when we decrease the number of measurements, however, with nine indentations it is still possible to see the two subpopulations (Figure 2).

We extracted the spring constant from every force curve we obtain with the automated procedure. Based on the results published by El-Kirat-Chatel[42] a shift on the results for the treated cells with respect to the native cells was expected, these can be confirmed by looking at Figure 2 (A and C, B and D). On the contrary, the presence of the two peaks in the histograms that we observed in all four experiments were unexpected. Indeed, experiments performed on single cell[(24,42)]only demonstrated homogeneous distribution of the nanomechanical properties. The difference in the spring constant absolute value for the two independent experiments on native cells may come from uncontrollable differences in the cell cultures. Indeed, the maximum applied force, the tip velocity, the cantilever spring constant, the buffer, the temperature, etc were the same. It is important to note that *C. albicans* is actually an extremely versatile microbe[43] able to sense and adapt to its environment. As a consequence, the growth phases of *C. albicans* are difficult to control and an unmeasurable difference in the initial culture conditions may result through the butterfly effect to the difference that we observe in between experiment 1 and 3. A further interesting experiment would be to follow a cell culture in order to monitor it's evolution throughout the time. But, most importantly we reproduced, two times, the distribution of the cells into two distinct populations. Dague E. et.al[44] reported an heterogeneity on the young modulus of *Saccharomyces cerevisiae* cells analyzed in the same conditions. Nevertheless, the numbers were really low (5 cells) and it was therefore impossible to draw a general conclusion at the population scale. Sub-populations in *C. albicans* have been described since more than ten years in the context of biofilms. They are reported to be responsible of biofilm resistance to chelating agents[45] and to antifungal drugs like amphotericin B[46]. In this last publication, the authors demonstrated that the sub-population was associated to ergosterol and beta 1-6 glucan pathway genes. They both are important component of the fungal cell wall and we know from previous investigation of the team[47] that their expression level is correlated with the nanomechanical properties of the cells. More recently, Rosenberg et al. showed that antifungal tolerance was a sub-population effect[48]. It therefore seems that sub-populations in *C. albicans* are common. In our work there is no a particular reason responsible for the 2 sub-populations, and we must admit that we have no clue of its origin. Globally, we can hypothesize that sub-populations, in *C. albicans* are an adaptation mechanism probably responsible for the remarkable expansion of this microbe, usually being commensal but also opportunistic pathogen.

To our knowledge this work is the first that reports the use of AFM to analyze hundreds of cells which demonstrate that a microbe population is mechanically heterogeneous. Supp Figure S6. (A and B) show the presence of the two populations at all times during the experiment. This means that the sub-populations are not due to the alteration or modification of the cells during the experiments. The two populations exist from the beginning to the end of the experiments. We also wondered if the sub populations could be due to an artifact linked with the tip position above the cell/well. To eliminate this hypothesis, we examined the distribution of stiffness constants for each position of the tip. This analysis, presented in Figures S6C and S6D (supp. Figure S6.), shows that the spring constants are distributed according to the same sub-population distribution for each analysis point. There is, therefore, no one position category that contributes to one sub-population and another position category that contributes to the other sub-population. These subpopulations are really linked to differences in spring constant between cells and are really reflecting the biological reality, complexity, variability of a *Candida albicans* cell population.

To be sure we also calculated the average value of each cell and represented these values on a histogram (supp. Figure S5). These representations show 2 sub-populations, centered on the same values as those of the global distribution histograms.

Our strategy to achieve a few force curves (9 to 16) over a large number of cells marks a break with the traditional approach to mechanical measurements, by AFM, on living cells. Nevertheless, we compared our results with those in the literature to validate the approach. Indeed, if the measurement on hundreds of cells were theoretically to open the door to the observation of sub-population, the decrease in the number of force curves, per cell, may also have negative effects. El Kirat-Chatel et.al[42] performed 256 nanoindentations on single cell, they found a stiffness value of 51+/-9 pN/nm for cells not treated with caspofungin and 27+/-10 pN/nm for cells treated with caspofungin. Our results are of the same order of magnitude (spring constant ranging from 21+/-6 to 81+/-19 pN/nm for native cells) and we observe the same tendency to decrease the spring constant with caspofungin treatment (spring constant ranging from 13 to 52 pN/nm, in our experiments, for caspofungin treated cells).

In another paper by Formosa et.al[24] showed that *Candida albicans* cells treated with caspofungin became harder. Formosa results are based on the analysis of 1024 nanoindentations performed on a cell. This inconsistency could be explained if authors selected an untreated cell from the softest subpopulation and a treated cell from the hardest subpopulation. Having no means at that time to access the sub-populations, the 2 results were accurate but incomplete. These inconsistencies are numerous in the literature and have partly motivated our work.

The results of the adhesion measures are particularly interesting and highlight the limit with which our method could be confronted. Indeed, it is known that *Candida albicans* is able to express on its surface a large number of different adhesins, in variable quantities[43,49]. The conditions of expression of some of them are known but for example the conditions of amyloid aggregation described in[41] have not been demonstrated. It seems that it could be triggered by mechanical stimulation (force induced nanodomain Alsteens PNAS ALS5[50]) but this has not been demonstrated in *Candida*. Our adhesion results are different from one experiment to another, although the culture conditions were

the same or at least we had the impression that they were the same, the usual microbiological techniques being implemented. This probably means that the expression of adhesins and or their organization on the cell surface in experiments 1 and 2 were different. Our method is not designed to analysis in high details single cells and therefore the detection of nanodomains is impossible. It means that the traditional approach is not antagonist with our new method and that they provide additional information. Moreover, the differences in spring constant between the nanodomains and the "normal" cell wall are not in the order of magnitude of the 2 sub-populations. Stiffer nanodomains are 13.4 +/- 0.2 nN/µm when the rest of the cell wall is 12.4 +/- 0.3 nN/µm[41]. In the present work we report a sub-population at 21+/- 6 nN/µm and the second at 48 +/- 9 nN/µm. It means that the difference due to the nanodomains are included in the error bar of our measurement.

Thus, and that is a potential new limit, our results would no longer be incomplete because they would not consider the heterogeneity of the cell population but incomplete because we would lack control over the biological sample produced. *Candida albicans* is known for its versatility[43] and in this context serves this demonstration better than any other cell model would have done.

Conclusions

An automated methodology for AFM force curves acquisition on cell population was successfully developed and implemented on a JPK Nanowizard II. The portability of the algorithm was tested on a JPK Nanowizard III. The results demonstrate that increasing drastically the number of cells analyzed (from tens to hundreds) makes it possible to describe a cell population from the nanomechanical point of view. Moreover, we showed that the number of measurements per cell has no impact on the significance of the result.

Our results, in addition to being consistent with those in the literature, show for the first time the presence of at least 2 subcellular populations. These are distinguished by differences in mechanical properties and cell wall adhesion. This discovery could have important implications for understanding the pathogenicity of *Candida albicans*. Indeed, the adhesion of cells to the host represents the first stage of infection and the mechanical environment of *Candida* is known to induce transformation from the yeast form to the invasive hypha form. Different subpopulations in terms of adhesion and mechanical properties are thus potentially responsible for one or the other of these key stages of *Candida albicans* infection.

Methods

Cell culture

The cell cultures were prepared as previously reported[24,41]. *C. albicans* was stored at -80°C, four independent cultures were prepared with the *C. albicans* revivified on Yeast. Peptone Dextrose (YPD) agar, and each were grown in 5 ml YPD broth for 20 h at 30°C under static conditions. In two of these four independent cultures 9.4 µl of caspofungin at 0.1 mg/ml (4xMIC) concentration were added and let under static conditions for 24 h at 30°C. Yeast cells (native and treated) were concentrated by centrifugation, washed two times in acetate buffer, and resuspended in acetate buffer just before performing AFM experiments.

Sample preparation

600 µL were taken from the resuspended cell solution and centrifuged, to separate the buffer from the cells. The supernatant is deposited onto a PDMS stamp, prepared as described in[38] and degassed for about 40 min. After 40 min. the buffer is removed from the PDMS surface, 200 µl of the cells solution are deposited and allowed to stand for 15 min. at room temperature. The cells were then placed into the microstructures of the stamp by convective/capillary assembly as described in[38].

The PDMS stamp with cells was finally fixed on a Petri dish (FluoroDish FD35-100) and it was filled with 5 ml of acetate buffer solution to maintain the cells in liquid media.

AFM measurements

For all experiments, commercially available silicon nitride triangular cantilevers (Bruker MLCT) with spring constants and sensitivity ranging respectively from 0.0110 N/m to 0.0405 N/m and from 31.8 nm/V to 54.2 nm/V were used. Cantilevers were calibrated using the thermal tune method. The parameters used to engage the tip on the stamp surface were as follows: IGain= 70 Hz, PGain= 0.002, Setpoint=0.559 nN. The topographic image used to determine W1 and W2 coordinates was recorded in the force map mode, (64 x64 pixels, maximum applied force 1nN, tip velocity 10 $\mu m.s^{-1}$). The maximum applied force used to record force curves was set to 1 nN and the piezo and motor stage speed were 10 µm/s and 200 µm/s respectively. The AFM field was 10,000 μm^2 (100 µm x 100 µm).

The AFM automation has been implemented on a JPK Nanowizard II, with a motorized precision stage MotStage Zeiss AxioObserver (S/N SM-01-0017) on an inverted optical microscope Zeiss Axiovert 200M. The AFM control software (SPM version 4) runs under Ubuntu 10.04 LTS (Lucid Lynx), the script was executed by using the experiment planner module, included in the JPK SPM software control. Indeed, the experiment planner mode offers a Jython scripting interface to control the AFM, hence the software programs for automation has been developed in Jython programming language.

Statistical analysis: k-means method

The k-means method has been used to group the subpopulations observed in the results. The method is based in the Hartigan and Wong algorithm[39], it divides M points in N dimensions into K clusters, the clusters centers are at the mean of their Voronoi set[40] (the set of data points which are nearest to the group center). The procedure is to minimize the within-cluster sum of squares so the dimension of the clusters will be changed until the items in the same cluster are similar as possible and items in different clusters are different as possible.

The k-means method was used to divide the stiffness and adhesion results into groups for analysis.

Authors contribution

E. Dague and A. Martínez-Rivas designed the research and experiments. S. Proa-Coronado and C. Séverac wrote the automation program. S. Proa-Coronado, C. Séverac, and E. Dague made the experiments. All the authors contributed to the writing and critical proofreading of the manuscript.

The authors declare no conflict of interest. This paper is not submited elsewhere and has not been considered for publication in any other journal.

Conflicts of interest

There are no conflicts to declare.

Acknowledgements

We want to acknowledge FONCYCYT of CONACYT (Mexico), the ministry of Foreign affairs of France and the Université Paris 13, though the financial support of the international collaborative ECOS-NORD project named Nano-palpation for diagnosis, No. 263337 (Mexico) and MI5P02 (France). AMR would like to thank the financial support of SIP-IPN through the project No. 20195489. SPC is supported by a PhD fellowship from CONACYT (No. 288029) and IPN through the cotutelle agreement to obtain double PhD certificate (IPN-UPS). ED is researcher at Centre National de la Recherche Scientifique (CNRS).

References

1. *E. M. Darling and D. Di Carlo, Annu. Rev. Biomed. Eng., 2015, 17, 35–62.*
2. *S. E. Cross, Y.-S. Jin, J. Rao and J. K. Gimzewski, Nat. Nanotechnol., 2007, 2, 780–783.*
3. *K. S. Kim, C. H. Cho, E. K. Park, M.-H. Jung, K.-S. Yoon and H.-K. Park, PLOS ONE, 2012, 7, e30066.*
4. *M. Plodinec, M. Loparic, C. A. Monnier, E. C. Obermann, R. Zanetti-Dallenbach, P. Oertle, J. T. Hyotyla, U. Aebi, M. Bentires-Alj, R. Y. H. Lim and C.-A. Schoenenberger, Nat. Nanotechnol., 2012, 7, 757–765.*
5. *M. Lekka, P. Laidler, D. Gil, J. Lekki, Z. Stachura and A. Z. Hrynkiewicz, Eur. Biophys. J., 1999, 28, 312–316.*
6. *M. E. Grady, R. J. Composto and D. M. Eckmann, J. Mech. Behav. Biomed. Mater., 2016, 61, 197–207.*
7. *R. Omidvar, M. Tafazzoli-shadpour, M. A. Shokrgozar and M. Rostami, J. Biomech., 2014, 47, 3373–3379.*
8. *L. Bastatas, D. Martinez-Marin, J. Matthews, J. Hashem, Y. J. Lee, S. Sennoune, S. Filleur, R. Martinez-Zaguilan and S. Park, Biochim. Biophys. Acta BBA - Gen. Subj., 2012, 1820, 1111–1120.*
9. *G. Smolyakov, B. Thiebot, C. Campillo, S. Labdi, C. Severac, J. Pelta and É. Dague, ACS Appl. Mater. Interfaces, 2016, 8, 27426–27431.*
10. *M. G. Haugh, C. M. Murphy, R. C. McKiernan, C. Altenbuchner and F. J. O'Brien, Tissue Eng. Part A, 2010, 17, 1201–1208.*
11. *Alibert Charlotte, Goud Bruno and Manneville Jean-Baptiste, Biol. Cell, 2017, 109, 167–189.*
12. *Y.-Q. Chen, C.-W. Chen, Y.-L. Ni, Y.-S. Huang, O. Lin, S. Chien, L. A. Sung and A. Chiou, J. Biophotonics, 7, 647–655.*
13. *A. F. Guedes, F. A. Carvalho, I. Malho, N. Lousada, L. Sargento and N. C. Santos, Nat. Nanotechnol., 2016, 11, 687–692.*
14. *J. Domke, W. J. Parak, M. George, H. E. Gaub and M. Radmacher, Eur. Biophys. J. EBJ, 1999, 28, 179–186.*
15. *G. Genet, C. Guilbeau-Frugier, B. Honton, E. Dague, M. D. Schneider, C. Coatrieux, D. Calise, C. Cardin, C. Nieto, B. Payré, C. Dubroca, P. Marck, C. Heymes, A. Dubrac, D. Arvanitis, F. Despas, M.-F. Altié, M.-H. Seguelas, M.-B. Delisle, A. Davy, J.-M. Sénard, A. Pathak and C. Galés, Circ. Res., 2012, 110, 688–700.*
16. *Y. Liu, J. Feng, L. Shi, R. Niu, Q. Sun, H. Liu, J. Li, J. Guo, J. Zhu and D. Han, Nanoscale, 2011, 4, 99–102.*
17. *W. S. Yoshikawa, K. Nakamura, D. Miura, J. Shimizu, K. Hashimoto, N. Kataoka, H. Toyota, H. Okuyama, T. Miyoshi, H. Morita, K. F. Kusano, T. Matsuo, M. Takaki, F. Kajiya, N. Yagi, T. Ohe and H. Ito, Circ. J., 2013, 77, 741–748.*
18. *J. C. Benech, N. Benech, A. I. Zambrana, I. Rauschert, V. Bervejillo, N. Oddone and J. P. Damián, Am. J. Physiol.-Cell Physiol., 2014, 307, C910–C919.*
19. *E. Dague, G. Genet, V. Lachaize, C. Guilbeau-Frugier, J. Fauconnier, C. Mias, B. Payré, L. Chopinet, D. Alsteens, S. Kasas, C. Severac, J. Thireau, C. Heymes, B. Honton, A. Lacampagne, A. Pathak, J.-M. Sénard and C. Galés, J. Mol. Cell. Cardiol., 2014, 74, 162–172.*
20. *A. B. Mathur, A. M. Collinsworth, W. M. Reichert, W. E. Kraus and G. A. Truskey, J. Biomech., 2001, 34, 1545–1553.*
21. *C. Formosa-Dague, R. E. Duval and E. Dague, Semin. Cell Dev. Biol., 2018, 73, 165–176.*
22. *G. Francius, O. Domenech, M. P. Mingeot-Leclercq and Y. F. Dufrêne, J. Bacteriol., 2008, 190, 7904–7909.*
23. *C. Feuillie, C. Formosa-Dague, L. M. C. Hays, O. Vervaeck, S. Derclaye, M. P. Brennan, T. J. Foster, J. A. Geoghegan and Y. F. Dufrêne, Proc. Natl. Acad. Sci., 2017, 114, 3738–3743.*
24. *C. Formosa, M. Schiavone, H. Martin-Yken, J. M. François, R. E. Duval and E. Dague, Antimicrob. Agents Chemother., 2013, 57, 3498–3506.*
25. *M. Li, N. Xi, Y. Wang and L. Liu, Nano Res., , DOI:10.1007/s12274-018-2260-0.*
26. *B. Nathwani, W. M. Shih and W. P. Wong, Biophys. J., 2018, 115, 2279–2285.*
27. *G. Binnig, C. F. Quate and Ch. Gerber, Phys. Rev. Lett., 1986, 56, 930–933.*

28. H. Schillers, C. Rianna, J. Schäpe, T. Luque, H. Doschke, M. Wälte, J. J. Uriarte, N. Campillo, G. P. A. Michanetzis, J. Bobrowska, A. Dumitru, E. T. Herruzo, S. Bovio, P. Parot, M. Galluzzi, A. Podestà, L. Puricelli, S. Scheuring, Y. Missirlis, R. Garcia, M. Odorico, J.-M. Teulon, F. Lafont, M. Lekka, F. Rico, A. Rigato, J.-L. Pellequer, H. Oberleithner, D. Navajas and M. Radmacher, Sci. Rep., 2017, 7, 5117.

29. I. Sokolov, M. E. Dokukin and N. V. Guz, Methods, 2013, 60, 202–213.

30. D. Di Carlo, J. Lab. Autom., 2012, 17, 32–42.

31. Martínez-Rivas, A., Dague, E., Proa-Coronado, S., Séverac, C. & González-Quijano, G. 2018 Patent: WO2019112414 (A1)—2019-06-13.
https://patentscope.wipo.int/search/es/detail.jsf?docId=WO2019112414&tab=PCTBIBLIO&maxRec=1000

32. Z. Wang, L. Liu, Y. Wang, N. Xi, Z. Dong, M. Li and S. Yuan, J. Lab. Autom., 2012, 17, 443–448.

33. R. Roy, W. Chen, L. Cong, L. A. Goodell, D. J. Foran and J. P. Desai, IEEE Trans. Autom. Sci. Eng., 2013, 10, 462–465.

34. M. Favre, J. Polesel-Maris, T. Overstolz, P. Niedermann, S. Dasen, G. Gruener, R. Ischer, P. Vettiger, M. Liley, H. Heinzelmann and A. Meister, J. Mol. Recognit., 2011, 24, 446–452.

35. H. Sadeghian, R. Herfst, B. Dekker, J. Winters, T. Bijnagte and R. Rijnbeek, Rev. Sci. Instrum., 2017, 88, 033703.

36. A. Dujardin, P. D. Wolf, F. Lafont and V. Dupres, PLOS ONE, 2019, 14, e0213853.

37. Dague Etienne, Proa Coronado Sergio, Severac Childerick & Martinez Rivas Adrian. AUTOMATIP: Automation of Biophysical measurements on cells by Atomic Force Microscope (AFM). Copyright: 03-2017-113012552200-01. (Instituto Politecnico Nacional, 2017).

38. C. Formosa, F. Pillet, M. Schiavone, R. E. Duval, L. Ressier and E. Dague, Nat. Protoc., 2015, 10, 199–204.

39. J. A. Hartigan and M. A. Wong, J. R. Stat. Soc. Ser. C Appl. Stat., 1979, 28, 100–108.

40. R Core Team, R: A Language and Enviroment for Statistical Computing, R Foundation for Statistical Computing, Vienna, Austria, 2018.

41. C. Formosa, M. Schiavone, A. Boisrame, M. L. Richard, R. E. Duval and E. Dague, Nanomedicine Nanotechnol. Biol. Med., 2015, 11, 57–65.

42. S. El-Kirat-Chatel, A. Beaussart, D. Alsteens, D. N. Jackson, P. N. Lipke and Y. F. Dufrêne, Nanoscale, 2013, 5, 1105–1115.

43. D. Poulain, Crit. Rev. Microbiol., 2015, 41, 208–217.

44. E. Dague, E. Jauvert, L. Laplatine, B. Viallet, C. Thibault and L. Ressier, Nanotechnology, 2011, 22, 395102.

45. J. J. Harrison, R. J. Turner and H. Ceri, FEMS Microbiol Lett, 2007, 272, 172–181.

46. P. D. Khot, P. A. Suci, R. L. Miller, R. D. Nelson and B. J. Tyler, Antimicrobial Agents and Chemotherapy, 2006, 50, 3708–3716.

47. M. Schiavone, S. Déjean, N. Sieczkowski, M. Castex, E. Dague and J. M. François, Front. Microbiol., 2017, 8, DOI:10.3389/fmicb.2017.01806.

48. A. Rosenberg, I. V. Ene, M. Bibi, S. Zakin, E. S. Segal, N. Ziv, A. M. Dahan, A. L. Colombo, R. J. Bennett and J. Berman, Nature Communications, 2018, 9, 2470.

49. P. W. J. de Groot, O. Bader, A. D. de Boer, M. Weig and N. Chauhan, Eukaryot. Cell, 2013, 12, 470–481.

50. D. Alsteens, M. C. Garcia, P. N. Lipke and Y. F. Dufrêne, Proc. Natl. Acad. Sci., 2010, 107, 20744–20749.